

Research Paper

Cadmium isotope evidence for near-modern bio-productivity in the early Cambrian ocean

Zeyang Liu^{a,b,c}, Alexander J. Dickson^d, Haijing Sun^e, Yaowen Wu^{a,c}, Zhen Qiu^f, Hui Tian^{a,c,*}^a State Key Laboratory of Organic Geochemistry, Guangzhou Institute of Geochemistry, Chinese Academy of Sciences, Guangzhou 510640, China^b State Key Laboratory of Oil and Gas Reservoir Geology and Exploitation, Chengdu University of Technology, Chengdu 610059, China^c CAS Center for Excellence in Deep Earth Science, Guangzhou Institute of Geochemistry, Chinese Academy of Sciences, Guangzhou 510640, China^d Centre of Climate, Ocean and Atmosphere, Department of Earth Sciences, Royal Holloway University of London, Egham, Surrey TW20 OEX, UK^e State Key Laboratory of Palaeobiology and Stratigraphy, Center for Excellence in Life and Palaeoenvironment, Nanjing Institute of Geology and Palaeontology, Chinese Academy of Sciences, 210008 Nanjing, China^f Research Institute of Petroleum Exploration & Development, PetroChina, Beijing 100083, China

ARTICLE INFO

Editor: Vasileios Mavromatis

Keywords:

Cd isotopes
Ocean oxygenation
Cambrian explosion
Deep-water
Productivity

ABSTRACT

The Ediacaran–Cambrian transition was one of the major transitions in Earth's history, with mass extinctions and radiation of animals. This event has been linked with perturbations in ocean geochemistry, including redox conditions and the oxygenation of Earth's surface environments. Here we present a highly resolved cadmium isotope record ($\delta^{114}\text{Cd}$) from shales deposited in a deep-water environment covering the Late Ediacaran to Cambrian Stage 4. Our $\delta^{114}\text{Cd}$ data vary from -0.70 to $+0.35\%$ and demonstrate the importance of local redox-dependent burial phases on bulk sediment Cd isotope compositions, which are superimposed on global-scale changes in the Cd cycle. The heaviest Cd isotope composition recorded in the early Cambrian Liuchapo Formation is similar to the modern deep ocean, implying a broad similarity in global Cd cycling, perhaps involving similar organic-Cd burial rates. The provision of bio-limiting nutrients by continental weathering with rising oxygen concentrations in Earth's surface environments could have expanded the habitable area of the ocean and contributed to animal diversification.

1. Introduction

The Ediacaran–Cambrian period is a major changeover interval in Earth's history, marked by the radiation and extinction of marine animals and significant changes in ocean chemistry (Zhang and Shu, 2021). The Ediacaran Biota, consisting largely of soft-bodied and a few skeletal multicellular organisms of uncertain phylogenetic affinities, are globally distributed and marked by a great morphological diversity during 575–541 Ma. This distribution and diversity subsequently disappeared across the Ediacaran–Cambrian boundary (Droser and Gehling, 2015; Laflamme et al., 2013; Zhu et al., 2017), and was largely replaced by the explosive appearance of major animal phyla in the early Cambrian (Droser and Gehling, 2015). This rapid diversification and evolutionary event is thought to have been achieved within just ~ 20 million years (the Cambrian Explosion). The increased mobility and predatory behaviour of Cambrian animals would require a higher oxygen level in

the ocean and atmosphere (Sperling et al., 2013).

The disappearance of the Ediacaran Biota (Laflamme et al., 2013) has been attributed to a mass extinction driven by expanded ocean anoxic zones (Tostevin et al., 2019; Zhang et al., 2018), while the evolution of active, large body size animals with higher energy consumption has been attributed to the expanding oxygen reservoirs of the ocean and atmosphere (Sahoo et al., 2016; Wang et al., 2018). Nonetheless, redox-sensitive trace elements, iron speciation and sulfur isotopes indicate that anoxic/ferruginous deep waters were persistently present at some locations across the Ediacaran–Cambrian transition, particularly in the Yangtze Block of South China (Canfield et al., 2008; Och et al., 2013; Sperling et al., 2015). On the other hand, molybdenum and uranium isotope data indicate a stepwise increase in ocean oxygenation during the early Cambrian, perhaps to modern levels (Chen et al., 2015; Wei et al., 2018). These conflicting observations have been reconciled by suggestions of a stratified redox model for the Cambrian ocean, with

* Corresponding author at: State Key Laboratory of Organic Geochemistry, Guangzhou Institute of Geochemistry, Chinese Academy of Sciences, Guangzhou 510640, China.

E-mail address: tianhui@gig.ac.cn (H. Tian).

<https://doi.org/10.1016/j.chemgeo.2024.122275>

Received 27 March 2024; Received in revised form 29 June 2024; Accepted 9 July 2024

Available online 10 July 2024

0009-2541/© 2024 The Authors. Published by Elsevier B.V. This is an open access article under the CC BY-NC-ND license (<http://creativecommons.org/licenses/by-nc-nd/4.0/>).

oxygenated surface and deep waters bracketing a euxinic layer at mid-depths ('euxinic wedge') (Li et al., 2020). In addition to ocean redox conditions, the supply of bio-essential nutrients is crucial in controlling ocean primary productivity and animal evolution (Shields, 2016). Therefore, there is a need to reconsider the ocean nutrient cycles and understand their relations to ocean redox condition and primary productivity during the Ediacaran–Cambrian transitions.

Cadmium has a broadly similar behaviour to the macronutrient phosphorus in the modern ocean, with nutrient-like distributions in modern water masses (Bruland, 1980; Middag et al., 2018). Cadmium fluxes into the ocean have two primary sources: rivers ($\delta^{114}\text{Cd} = +0.1\%$ to $+0.3\%$) (Lambelet et al., 2013) and dust ($\delta^{114}\text{Cd} = -0.19\%$ to $+0.19\%$) (Bridgestock et al., 2017). Marine phytoplankton preferentially utilise isotopically light Cd, leaving surface waters with low Cd concentrations [Cd] and heavy isotope compositions (by up to $\sim +5\%$; Conway and John, 2015; Janssen et al., 2017; Janssen et al., 2014; Lacan et al., 2006; Ripperger et al., 2007; Sieber et al., 2019). In comparison, the modern deep ocean seawater is characterised by a $\delta^{114}\text{Cd}$ value of $0.25 \pm 0.04 \%$ that is isotopically heavier than the above mentioned inputs, but lighter than shallow waters due to the remineralisation of sinking organic material (Sieber et al., 2023). Cadmium is mainly removed from seawater by association with organic matter and authigenic Cd-sulfides in sub-oxic and anoxic sediments (Bryan et al., 2021; Chen et al., 2021; Plass et al., 2021). Organic matter is likely to be a primary phase that removes Cd into surface sediments, with Cd isotope values lighter than the overlying seawater (Bryan et al., 2021; Janssen et al., 2019). In the presence of free aqueous H_2S , the formation of CdS could also be significant (Bryan et al., 2021; Guinoiseau et al., 2019; Rosenthal et al., 1995). This process would result in elevated sedimentary [Cd] with isotope compositions approaching the overlying bottom ocean water, due to precipitation of Cd in porewaters derived from seawater diffusion and perhaps partial remineralisation from other sedimentary phases during shallow diagenesis (Bryan et al., 2021; Guinoiseau et al., 2018; Janssen et al., 2014). Other sedimentary sinks of Cd include Fe–Mn oxides (Rehkämper et al., 2012), with Cd isotopic values similar to deep seawater (Horner et al., 2011; Schmitt et al., 2009). This pathway may also be locally important when Fe-oxide precipitation-reduction occurs near the sediment-water interface (Chen et al., 2021). Incorporation of Cd into biogenic and inorganic carbonates has also been invoked, but this would be a rather minor removal pathway for Cd in the ocean (Druce et al., 2022; Horner et al., 2011).

Cadmium isotopes have recently been used to track ocean chemistry perturbations over key geological intervals (Dickson et al., 2022; Frederiksen et al., 2022b, 2024; Frei et al., 2020; Frei et al., 2021; Hohl et al., 2019; Sweere et al., 2020). In this study, Cd isotope compositions were measured on the Doushantuo, Liuchapo and Niutitang formations of South China representing the late Ediacaran to Cambrian Stage 4. The new data are used to investigate the link between ocean redox and nutrient cycling with mass extinction and animal radiation events.

2. Geological background

The Yangtze Block is bounded by the Red River Fault Zone to the southwest, and the Xianshuihe Fault Zone to the west, the Qinling–Dabie orogenic belt to the north, and the Cathaysia Block to the southeast (Fig. 1) (Charvet, 2013). The Yangtze Block developed from a rift basin (~ 800 Ma) into a passive continental margin basin (~ 550 Ma) during the Ediacaran–Cambrian (E–C) transition following the Neoproterozoic rifting events (Li et al., 1999; Jiang et al., 2003; Wang and Li, 2003; Condon et al., 2005; Zhang et al., 2005; Jiang et al., 2006). The western platform interior is characterised by shallow water carbonate depositional facies, which developed to deep-water slope-basin facies in the south-eastern area via a transitional belt (Fig. 1) (Steiner et al., 2001). Following a northwestern transgression in Cambrian Stage 2, the slope-basin deposition expanded into the entire Yangtze Block.

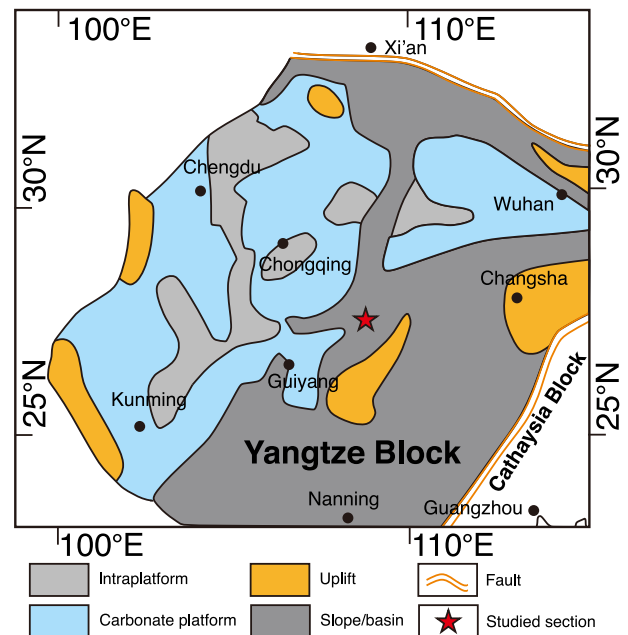


Fig. 1. Paleogeography map of the Cambrian Nanhua Basin and the location of the ZK4411 drill core (modified from Wu et al., 2022).

The core ZK4411 ($28^{\circ}02'32''$ N and $109^{\circ}04'33''$ E) was drilled in the Yinjiang county, ~ 270 km northeast of Guiyang City in South China and paleogeographically located in the slope region of the Yangtze Block during the E–C transition (Fig. 1; Wu et al., 2022). The lithology of the core includes the Upper Ediacaran Doushantuo Formation (Member IV), which consists of dolomite and shale. The Doushantuo Formation is overlain by the Liuchapo Formation that is dominated by cherts with thin layers of dolomite (~ 6 m) and organic-rich shale (~ 1 m) at the base. The overlying Niutitang Formation is mainly composed of black shale (~ 100 m) at the lower part and grey silty shale (~ 110 m) with several thin limestone layers at the upper part. A thin layer of polymetallic Ni–Mo sulphide ore (~ 0.5 m) is present at the base of the Niutitang Fm., which is usually used as a correlation horizon across the margin of the Yangtze Block (Jiang et al., 2007). The E–C boundary (~ 541 Ma) is placed at the bottom of the Liuchapo Formation coincident with a large negative carbon isotope excursion, which is typical of the basal Cambrian. Four stratigraphic intervals, designated as I to IV, have been established by using biostratigraphy and sedimentary sequences. These intervals represent significant periods of environmental changes and biological evolution. Interval I spans from the base of DST IV to the E–C boundary and is characterised by the extinction of the Ediacaran biota. Interval II is defined by the presence of the BACE (Base of Cambrian Stage) and the appearance of SSFAs (Small Shelly Fossils) during the Cambrian Fortunian to Age 2. Interval III predominantly consists of globally recognized transgressive black shales formed during the Cambrian Age 2–3. Interval IV is notable for the occurrence of the abundant Chengjiang Biota in the early to middle Age 3 of the Cambrian period. Correlations with other Ediacaran–Cambrian sections are made based on bio-, chem-, and litho-stratigraphy, as well as the marker layers (Fig. S1; Wu et al., 2022).

3. Samples and methods

Samples were collected over an interval of ~ 400 m, ranging from Late Ediacaran to Cambrian Stage 4, with sampling gaps of about 2 m (Table S1). Initial element concentrations, including Cd, were previously determined by total dissolution with a mix of $\text{HF-HNO}_3\text{-HClO}_4$ (28.9 M–15.6 M–11.7 M) and measured by Thermo Scientific Element XR ICP-MS with an external reproducibility of 7% (Table S1; Wu et al.,

2021, 2022). Aliquots of archived sample powders from core ZK4411 were subsequently weighed into Teflon digestion vessels together with a ^{113}Cd – ^{111}Cd double spike for isotopic determination. Precise spike/sample ratios were guided by previous Cd concentrations to obtain a spike: sample ratio of ~ 1.5 . Sample powders were digested on a hotplate at $150\text{ }^\circ\text{C}$ for 48–72 h in inverse aqua regia (iAR, $\text{HNO}_3\text{:HCl} = 3\text{:}1$) to preferentially dissolve authigenic shale components and minimize the digestion of detrital materials that generally contain negligible Cd. Cadmium was separated from major-element cations and interferences in a three-stage anion column chromatography procedure modified from previous studies (Sweere et al., 2020). The eluted samples were evaporated dry and redissolved in 1 mL of 3% HNO_3 before isotopic analyses. Stable-isotope analyses were performed on a Neptune Plus multi-collector ICP–MS at Royal Holloway University of London using 20 ng/g solutions aspirated via an Aridus III desolvator. Measurements consisted of 40 simultaneous 8.4-s integrations for ^{110}Cd , ^{111}Cd , ^{112}Cd , ^{113}Cd , ^{114}Cd , ^{115}In , ^{116}Cd and ^{117}Sn , with In and Sn used to correct for isobaric interferences. Each sample was preceded by a brief measurement of 3% HNO_3 , which was used to blank-correct the sample voltages.

Sample-spike mixtures were deconvolved offline using an Excel-based routine, incorporating corrections for Sn and In interferences. Isotope data were processed offline using an exponential mass-bias correction, and are expressed relative to the NIST-3108 Cd solution:

$$\delta^{114}\text{Cd} = \left[\frac{^{114}/^{110}\text{Cd}_{\text{sample}}}{^{114}/^{110}\text{Cd}_{\text{NIST}}} - 1 \right] * 1000.$$

Total procedural replicates of SGR-1b in the RHUL laboratory using the same methodology as used in this study yield a composition of 0.09 ± 0.06 per mil ($n = 9$). This is identical within uncertainties with other published values for this material (0.07 ± 0.05 , Tan et al., 2020; 0.05 ± 0.07 per mil and 0.06 ± 0.02 per mil, Zhong et al., 2023). An in-house reference material Kimmeridge Shale yielded a value of $\delta^{114}\text{Cd}_{\text{KIMM}} = +0.17 \pm 0.06\text{ }‰$ (2 SD, $n = 3$). This is a more precise determination of this material than Dickson et al. (2020), who reported a value of $+0.26 \pm 0.13\text{ }‰$ that is within uncertainty of the value reported here. Alfa Aesar Specpure Cd (‘OXCAD’), spiked similarly to samples, was measured in the same analytical sessions as the samples, yielding a value

of $-0.87 \pm 0.05\text{ }‰$ (2 S.D., $n = 15$) over the course of the study. This value is within uncertainty of the published value of $-0.81 \pm 0.1\text{ }‰$ (Abouchami et al., 2012). Reported uncertainties in Fig. 2 are the 2 standard error propagated uncertainties based on the reproducibility of the bracketing NIST standards and the internal error of each sample analysis. Cadmium concentrations were determined by isotope dilution using the $^{111}\text{Cd}/^{112}\text{Cd}$ ratio. Cadmium procedural blanks were ≤ 1.1 ng, accounting for $\leq 2\%$ of the Cd processed in the samples, so no blank corrections were applied.

4. Results

4.1. Cd concentrations

Cadmium concentrations in the in the non-detrital mineral leachates of the studied samples range from 0.01 to $117.46\text{ }\mu\text{g/g}$. For the Doushantuo samples, [Cd] increases sharply from $0.54\text{ }\mu\text{g/g}$ in the bottom of the section to $117.46\text{ }\mu\text{g/g}$, and then drop gradually across the E–C boundary to $0.01\text{ }\mu\text{g/g}$ in the lower Cambrian. Cd concentrations remain at slightly higher values (average $0.13\text{ }\mu\text{g/g}$, $n = 9$) in the Fortunian to Stage 2, and then increase to $6.16\text{ }\mu\text{g/g}$ in the Ni–Mo ore layer. The Cd values then decline to $0.73\text{ }\mu\text{g/g}$ in the lower Cambrian Stage 3. After a minor increase to $3.67\text{ }\mu\text{g/g}$, the [Cd] are then gradually reduced to $0.23\text{ }\mu\text{g/g}$ in the middle Cambrian Stage 3, followed by slightly higher values of 0.33 to $0.78\text{ }\mu\text{g/g}$ (average 0.56 , $n = 4$) in the interval of the uppermost Cambrian Stage 3 to lower Stage 4 (Fig. 2).

4.2. Cd isotopes

The Cd isotope compositions for core ZK4411 show great variations through the studied interval that range from -0.71 to $+0.35\text{ }‰$, with an average of $-0.04\text{ }‰$ ($n = 50$). In interval I, after an increase from $-0.01\text{ }‰$ to $+0.25\text{ }‰$ in the late Ediacaran period, Cd isotope compositions drop dramatically across the E–C boundary to a low value of $-0.49\text{ }‰$. After a small positive shift to $-0.16\text{ }‰$, Cd isotope compositions then drop further to the most negative value of $-0.71\text{ }‰$ in the middle of the

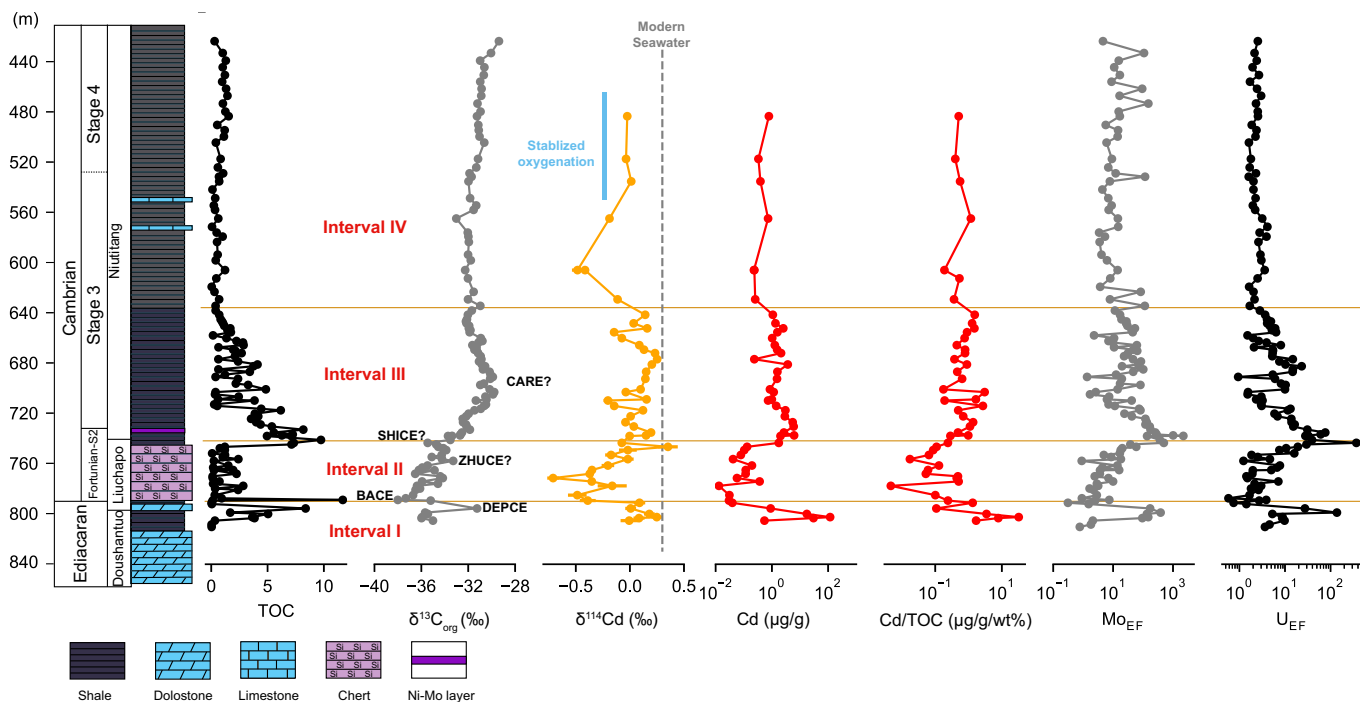


Fig. 2. Cd-isotope stratigraphy for the ZK4411 core. The $\delta^{13}\text{C}_{\text{org}}$ and TOC, Mo and U data are from Wu et al. (2022). DEPCE: DEngying Positive Carbon isotope Excursion; BACE: Basal Cambrian Carbon isotope Excursion; ZHUCE: ZHUjiaqing Carbon isotope Excursion; SHICE: SHIYantou Carbon isotope Excursion; CARE: Cambrian Arthropod Radiation isotope Excursion.

early Cambrian Liuchapo Fm. The lowest $\delta^{114}\text{Cd}$ observed in Interval II are considerably lower than dissolved $\delta^{114}\text{Cd}$ values generally found for the modern ocean. Samples from the E–C transition interval contain the lowest Cd isotope compositions and the lowest [Cd]. Cd isotope compositions then vary from +0.35 ‰ to –0.48 ‰ between the mid Fortunian to Stage 2 and the late Cambrian Stage 3, before reaching stable values of –0.02‰ ($n = 3$) in the early Stage 4 (Fig. 2).

5. Discussion

5.1. Evaluation of non-detrital Cd signatures in Nanhua basin sediments

The Cd concentration and isotope composition of sedimentary rocks could be potentially affected by detrital material and/or post-depositional alteration. No correlations between Cd or $\delta^{114}\text{Cd}$ with Al and Ti were found (Figs. 3A–D), which are frequently used as proxies for detrital components. Furthermore, [Cd] in detrital silicates are typically very low (Rudnick and Gao, 2003) and even if this fraction was fully liberated during the digestion procedure it would account for a minor part of the total Cd in most samples. Thus, we consider the Cd contribution from detrital materials is negligible in our samples. The samples have experienced high thermal maturation with equivalent vitrinite reflectance (EqVRo) ranging ~2.3–3.7% (Sun et al., 2023). However, laboratory pyrolysis experiments supported by field observations suggest that the thermal maturation of organic matter does not alter Cd

isotopic compositions significantly (Dickson et al., 2020, 2022). We therefore consider our Cd measurements to be unaffected by maturation artifacts.

5.2. Controls on sedimentary Cd enrichments

In sub-oxic/anoxic sediments, Cd is mainly hosted in organic matter and sulfides (Plass et al., 2020; Rosenthal et al., 1995). In a cross plot of Cd against total organic carbon (TOC), our samples largely show values above the typical Cd/C stoichiometry of ‘non-HNLC’ (high-nutrient low-chlorophyll) organic matter (Quay et al., 2015) (Fig. 4A). Samples that deviate strongly from HNLC Cd/C stoichiometries are also enriched in the sulfide-sensitive element molybdenum, supporting the role of CdS as a major host phase for these sampling intervals (Sweere et al., 2020).

Samples from Interval I generally have higher Cd isotope compositions (Fig. 4B), and five samples from this interval plot above the non-HNLC line in Fig. 4A, indicating a major host of CdS. On the other hand, samples from interval II have the lowest [Cd] and the lowest Cd/TOC ratios and mostly plot along or below the ‘non-HNLC’ line (Fig. 4A), which is consistent with organic matter acting as the main host of Cd deposited under less reducing conditions. This interpretation is consistent with lower Mo and U concentrations (Fig. 2, Table S1). Samples from Interval III largely plot above the ‘non-HNLC’ line in Fig. 3A, and their distribution in Cd/Mo versus Mn × Co space indicates their formation under hydrographically restricted conditions (Fig. 5). Therefore,

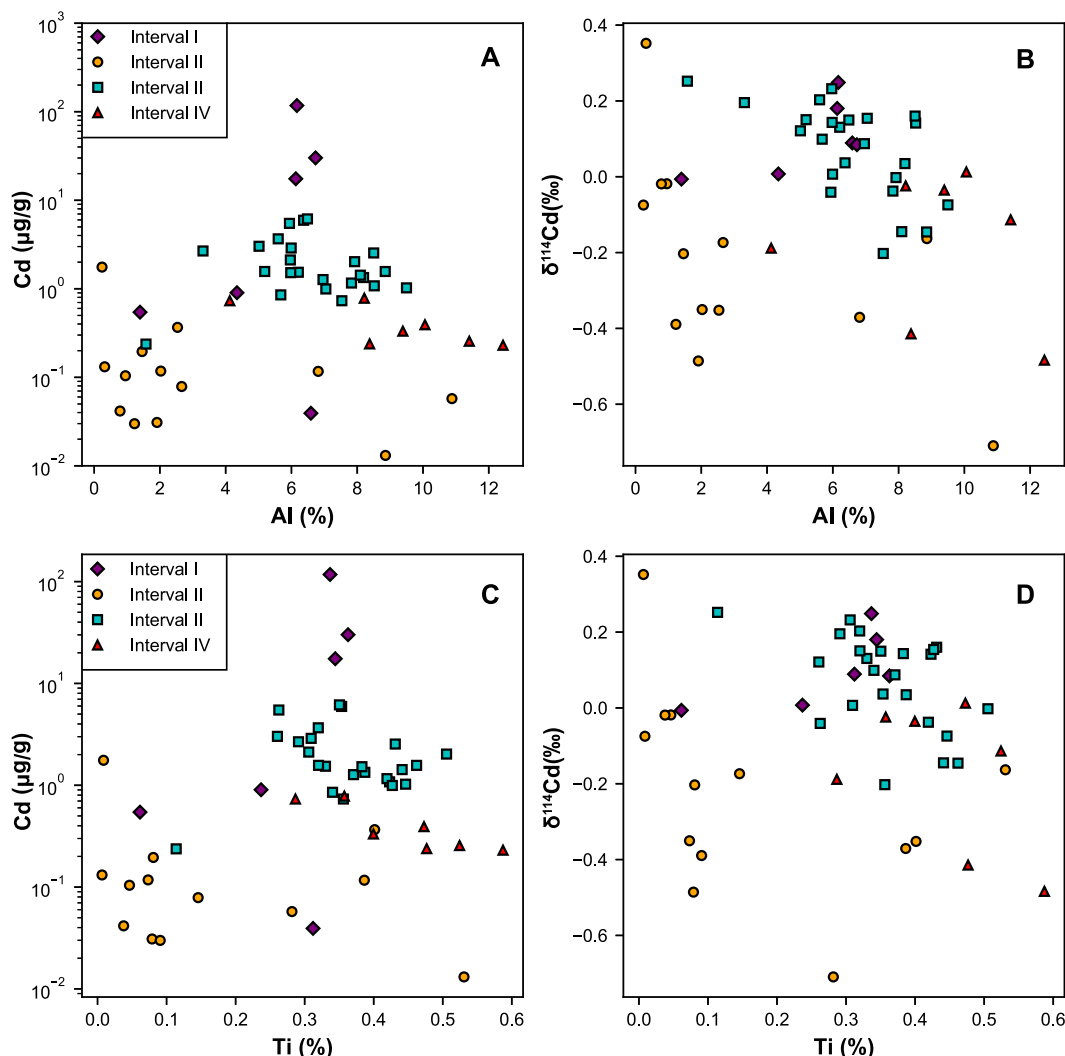


Fig. 3. Cross plots for Cd concentration and isotope composition against detrital influx proxies of Al and Ti concentrations (A–D).

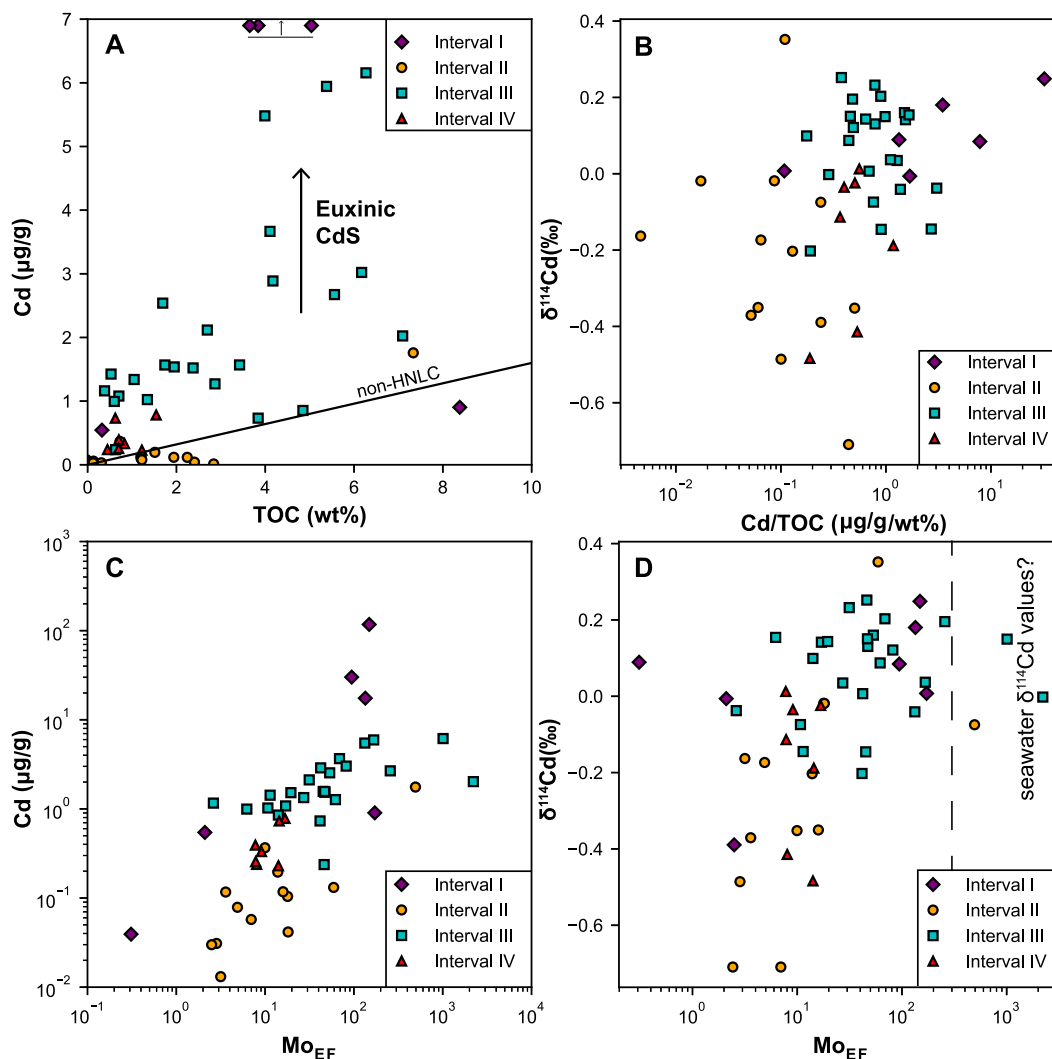


Fig. 4. Cross plots for Cd concentration against Mo_{EF} (A); $\delta^{114}Cd$ against Mo_{EF} (B); Cd concentration and TOC (C); $\delta^{114}Cd$ and Cd/TOC (D). The solid line denoting ‘non-HNLC’ (high-nutrient low-chlorophyll) represents the Cd/P ratios estimated for exported particles in non-HNLC ratios based on dissolved Cd and P patterns of Cd/P = 0.21 mmol/mol (Quay et al., 2015), which were then converted to Cd/TOC using a P:C ratio of 1:124 (Ho et al., 2003).

CdS is suggested to be the major host phase in the Interval III deposits. In Interval IV, samples are characterised by moderate [Cd] and Cd/TOC values, plot close to the ‘non-HNLC’ line (Fig. 4A), and have low and uncorrelated Mo_{EF} (Fig. 4C, Table S1), indicating that the major host for Cd is probably organic matter.

Basin restriction during intervals I and III may have been a key control on Nanhua Basin seawater [Cd] due to the cutoff of Cd supply from the open ocean. Hydrographic restriction over the Yangtze platform has been proposed by several studies for the Cambrian Fortunian and Age 2 (Och et al., 2016; Wu et al., 2021). In contrast, the Cd/Mo vs Co \times Mn cross-plot suggests a good connection with the open ocean for intervals II and IV (Figs. 2 and 5), an argument supported by unradiogenic initial Os isotope compositions of ~ 0.35 for the Liuchapo Formation deposits in Interval II (Wu, 2021). These unradiogenic values are distinct from the generally radiogenic Os isotope values that typify lacustrine depositional settings and restricted marine basins, where Os is dominated by riverine inputs from weathering of the ancient continent (e.g., $^{187}Os/^{188}Os$ of ~ 1.1 from the lacustrine Eocene Green River Formation, Unita Basin, USA; Cumming et al., 2012). Other evidence for a good connection with the open ocean in intervals II and IV includes the appearance of globally dispersed acritarchs *Protohertzina* and *Mongolodus* (Liu et al., 2013; Yi et al., 2022), the coherent and gradual temporal $\delta^{34}S_{py}$ trends (Sahoo et al., 2016), and carbon and strontium isotope

profiles from the Yangtze Platform that are globally correlative (Xiang et al., 2017). Paleogeographic reconstructions suggest that during the Ediacaran–Cambrian transition, the Yangtze Block was an independent continent surrounded by oceans (Jiang et al., 2003). A recent study suggests that the South China-Indochina block (including the Yangtze Block) and NW India block began to collide during 560–540 Ma (Yang et al., 2020). Therefore, local restrictions could happen in the proximal intrashelf basins, but not for the slope-basin environments (Jiang et al., 2011). The marine basins located in the southeast side of the Yangtze platform (including the studied section) could have been well-connected with the global ocean (Fig. 1).

5.3. Controls on Cd isotope fractionation in Nanhua basin sediments

The deposition of the Liuchapo chert (Interval II) during the early Cambrian has been suggested to be linked with increased silica input from hydrothermal fluids (Fan et al., 2013). Exhalative systems have been reported to be characterised with a mean $\delta^{114}Cd$ value of $0.12 \pm 0.50\%$ (Wen et al., 2016). A mean Cd isotope value of $-0.06 \pm 0.03\%$ (2SD) for the bulk silicate Earth has been reported recently (Pickard et al., 2022), which might be used to represent the hydrothermal fluid Cd isotope composition, assuming equilibration with hot oceanic crust. In addition, hydrothermal Cd inputs are considered to be minor

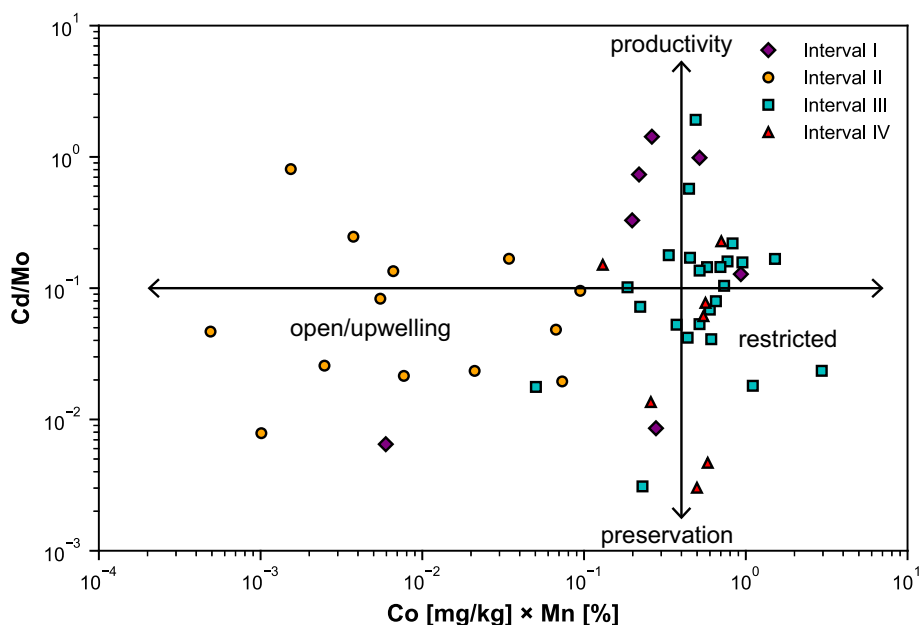


Fig. 5. Cd/Mo and Co \times Mn values for the Nanhua Basin sediments compared to values for modern organic-rich sediments from various environments following Sweere et al. (2016).

influences on seawater chemistry as they are largely deposited near the hydrothermal vent via CdS precipitation and act as a sink for Cd in the seawater cycle (Conway and John, 2015). The low Cd concentrations in the Liuchapo Formation are evidence against a large authigenic hydrothermal flux, which might be envisaged to push concentrations up.

In the absence of major perturbations to Cd inputs to the ocean and a changing deep ocean Cd isotope composition, $\delta^{114}\text{Cd}$ variations such as those observed here can largely be explained by changes in the fraction of Cd buried as different sedimentary phases, in particular CdS and/or organic matter. These flux changes are ultimately controlled by local redox variations that affect the stability of individual mineral phases, coupled with local primary productivity, diagenetic processes internal to the sedimentary succession and the basin seawater composition. A shift to more oxygenated conditions could have led to an overall larger isotopic offset between sediments and seawater via affecting the stability of many Cd-bearing phases such as oxyhydroxides, organic matter and sulphides, as shown in modern continental-margin sediments where oxic sediments have lower $\delta^{114}\text{Cd}$ values than those deposited in sub-oxic environments (Bryan et al., 2021). Larger seawater-sediment $\delta^{114}\text{Cd}$ offsets could be facilitated by an increase in the fraction of isotopically light Cd buried with organic matter, or possibly by the non-quantitative formation of CdS, with preferential precipitation of lighter Cd isotopes (Conway and John, 2015; Guinoiseau et al., 2018).

Samples from Interval I have $\delta^{114}\text{Cd}$ values that largely correlate with Cd/TOC ratios (Fig. 4B). The positive stratigraphic shift in $\delta^{114}\text{Cd}$ is correlative with an increase of both Mo_{EF} and U_{EF} , which might have been caused by an increasing fraction of CdS in the sedimentary environment. The shift to lower $\delta^{114}\text{Cd}$ over the E–C transition (interval I/II boundary) may therefore logically have been caused by the reverse process as more oxidizing conditions were established in the Nanhua basin. In this case, the low Mo_{EF} and U_{EF} values (Fig. 2, Table S1), which have previously been interpreted to represent basin restriction (Wu et al., 2021), could be re-interpreted to have been caused by limited enrichment under more oxidizing conditions. Interval III deposits are characterised by higher $\delta^{114}\text{Cd}$ values ($> -0.2\%$) and accumulation in a restricted oceanic setting (Figs. 2 and 5). In interval IV, samples are characterised by $\delta^{114}\text{Cd}$ values close to or $< 0\%$ and low Mo_{EF} and U_{EF} values, with no linear relationship between $\delta^{114}\text{Cd}$ and Cd/TOC. This observation could indicate a stable redox condition in the deep-water of the Nanhua basin.

The brief shifts to lower $\delta^{114}\text{Cd}$ within intervals III and IV might suggest either short-term decreases in CdS burial, and/or non-quantitative CdS formation. A decrease in CdS burial is supported by coeval depletion in [Cd], although either option would suggest a short-term change in the local basin redox conditions towards slightly more oxygenated environments.

5.4. Seawater Cd isotope compositions

We have noted that the sediment Cd isotope compositions frequently shift to values close to modern deep water (Fig. 2, $+0.25 \pm 0.05\%$ in Interval I, $+0.35 \pm 0.09\%$ in Interval II, and $+0.25 \pm 0.03\%$ in Interval III). We assume that the samples with high [Mo] concentrations, whose Cd/C ratios deviate to values higher than the stoichiometric relationship observed in modern plankton (Ho et al., 2003) contain Cd dominantly sourced from CdS precipitation. In this case and following observations from modern ocean sediments (Bryan et al., 2021), we interpret the highest isotope compositions of these samples as being close to coeval seawater, with a value of $\sim +0.28 \pm 0.12\%$ (2 S.D., $n = 3$, highest values from each of intervals I–III). This value overlaps the estimated seawater $\delta^{114}\text{Cd}$ value of $+0.35 \pm 0.10\%$ from the Niutitang Formation (Frei et al., 2020, 2021), estimated seawater $\delta^{114}\text{Cd}$ values from the Dengying and Zhujiqing formations of the Xiaotan Section (Fig. 6) (Frederiksen et al., 2022b), and the Niutitang Formation of the Zhongnancun section (inferred from authentic carbonate Cd isotope values) (Hohl et al., 2019) and the modern deep ocean water ($+0.25 \pm 0.04\%$) (Sieber et al., 2023). It is also identical to the $\delta^{114}\text{Cd}$ value of $+0.28 \pm 0.11\%$ estimated for early Cenomanian seawater (Sweere et al., 2020).

An early Cambrian Cd cycle similar to modern would imply that the global burial fractions of organic carbon-Cd and CdS were probably similar to today (Frederiksen et al., 2022b; Frei et al., 2020; 2021; Hohl et al., 2019). This observation also implies comparable availability of nutrients in the early Cambrian ocean to fuel biologic production (Frederiksen et al., 2022b; Frei et al., 2020; 2021; Hohl et al., 2019; Wang et al., 2018), although in contrast to some studies that suggest ‘modern’ like oxidative weathering of the continents occurred much later in the Paleozoic (Tostevin and Mills, 2020). The nutrient enrichment of surface waters during the Ediacaran–Cambrian transition may be directly linked to the enhanced weathering of ancient land masses

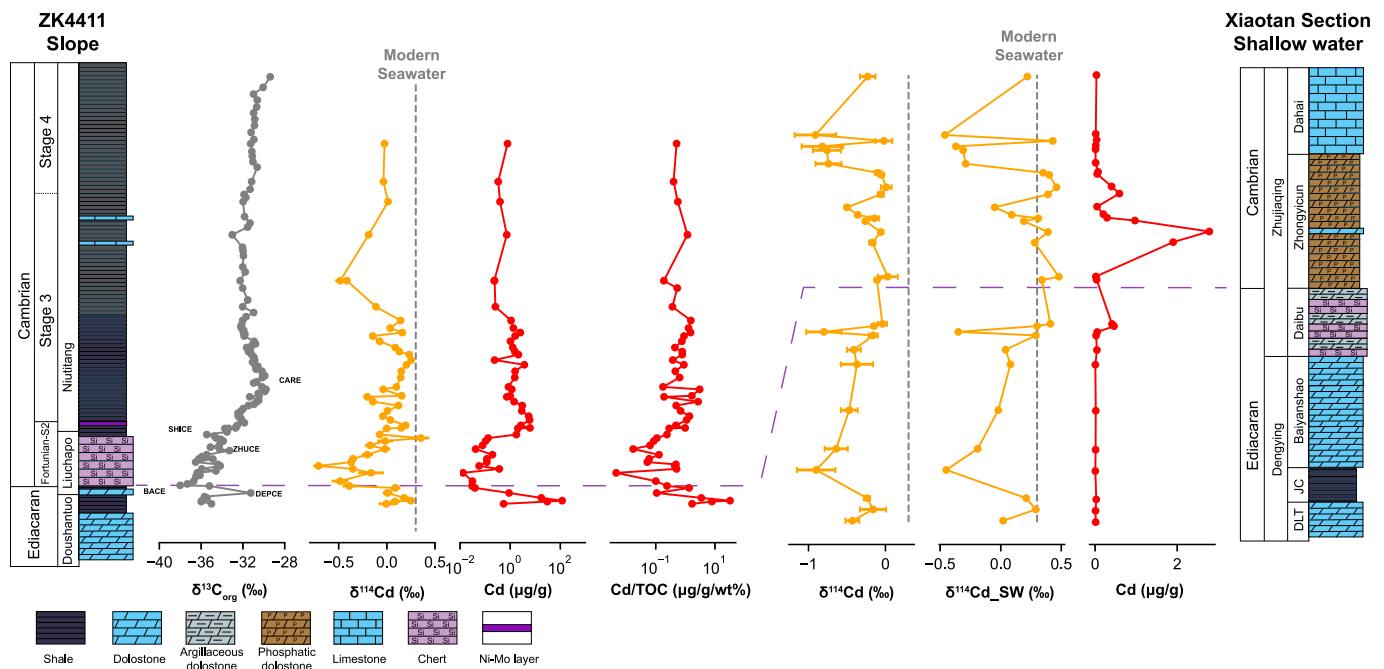


Fig. 6. Correlation of the Cd data from the ZK4411 core and the Xiaotan section (Frederiksen et al., 2022b). $\delta^{114}\text{Cd}_{\text{SW}}$ represents the seawater Cd isotope values inferred from carbonate $\delta^{114}\text{Cd}$ by Frederiksen et al. (2022b). DLT = Donglongtan, JC = Jiucheng.

(Brasier and Lindsay, 2001; Squire et al., 2006). As such, the elevated nutrient levels and enhanced bioproductivity may have led to heavy Cd isotopes in the surface seawaters of the Yangtze platform during the E–C transition due to the light Cd isotope uptake via primary producers. The fact that a deep seawater composition is similar to modern implies a correspondingly similar distribution of Cd burial fluxes (including in organic matter) globally. In addition, near-modern productivity levels have also been inferred from P, Ba and TOC related productivity proxies from the drill-core ZK107 (Songtao County, northeastern Guizhou Province, South China; Zhao et al., 2023).

It is interesting to note that one sample from the Ni–Mo layer (737.35 m) has a Mo_{EF} value of 1009 and a $\delta^{114}\text{Cd}$ value of $+0.15 \pm 0.04$ ‰ (Table S1). This value is lighter than the value of $+0.35 \pm 0.10$ ‰ ($n = 7$; 2 S.D.) reported by Frei et al. (2020, 2021) for the Huangjiawan mine (Zunyi, Guizhou province) and Sancha mining districts (including Sancha and Xiongjiata, about 25 km southwest of Sancha, Hunan province), or with two $\delta^{114}\text{Cd}$ values of $+0.35$ ‰ and $+0.41$ ‰ measured on selective dissolution of sulphides of similar Ni–Mo rich shales of the Niutitang Formation from the Zhongnancun section by Hohl et al. (2019). In theory $\delta^{114}\text{Cd}$ values in euxinic environments may reflect near-quantitative removal of Cd from seawater, as assumed by Hohl et al. (2019) and Frei et al. (2020, 2021), which linked the anomalously high metal contents in the Ni–Mo layer in these sediments with high bio-productivity in the surface waters. Hydrothermal origin for these metals have been also suggested (e.g., Jiang et al., 2007), however, as previously mentioned, hydrothermal sources of Cd have a variable Cd isotope composition (e.g., 0.12 ± 0.50 ‰ for the exhalative systems; Wen et al., 2016; -0.06 ± 0.03 ‰ for the bulk silicate Earth; Pickard et al., 2022), and are readily deposited nearby hydrothermal vents and considered as a sink for Cd (e.g., Conway and John, 2015). We note that the polymetallic sulfide layer in the studied section is different from other parts of the early Cambrian Yangtze platform, where Mo and Cd concentrations are much higher (Mo in the percent range and Cd in the tens of $\mu\text{g/g}$ range; e.g., Lehmann et al., 2007, 2016). As such, the lighter Cd isotope values of the Ni–Mo layer in this study could be explained by less quantitative Cd removal from anoxic or weakly sulfidic bottom water and sediment pore water, which may occur in temporally and spatially fluctuating paleoceanographic conditions in a marginal

basin on the early Cambrian Yangtze Platform. Similar conclusions have also been drawn based on Mo and U isotope studies on this Ni–Mo layers (e.g., Xu et al., 2023).

5.5. Implications for animal evolution

The mass extinction of the Ediacaran biota has been linked with intensive ocean anoxia in shallow-water environments, with evidence from redox proxies such as U and Mo isotopes (Tostevin et al., 2019; Wen et al., 2011; Zhang et al., 2018). Here we show that the deep water of the Cambrian Nanhua basin may have also experienced an expansion of ocean euxinia, which is consistent with our Cd isotope data, with a rapid shift from -0.01 ± 0.08 ‰ to more positive values of $+0.25 \pm 0.05$ ‰ in the upper interval I (at the top of the Doushantuo Fm, Fig. 2), ostensibly as a result of locally enhanced burial of CdS. This inference is consistent with the shift of Mo isotope compositions to heavier values in the latest Ediacaran (e.g., Wu et al., 2021).

Shortly after the latest Ediacaran, our new $\delta^{114}\text{Cd}$ data provide evidence of deep-water oxygenation in the Nanhua basin at the Ediacaran–Cambrian boundary. This oxygenation event is followed by repeated cycles of Cd isotope variations reflecting episodic expansion and contraction of bottom-water anoxia/euxinia in the basin. This pattern of stepwise oxygenation is similar to those inferred from coupled behaviour of the carbon and sulfur cycles at shallow-water carbonate sections (He et al., 2019), although stratigraphic uncertainties preclude any direct correlation of the data. If truly coeval, the various lines of evidence could suggest coeval oxygenation of the deep and shallow ocean.

The Cambrian radiation of animals has been linked with elevated nutrient levels, which could have boosted marine productivity (Shields, 2016; Wang et al., 2018). Our inferred deep-water Cd isotope values ($+0.28 \pm 0.12$ ‰) allow us to propose a paleo-Cd cycle that was similar to modern oceans, and by extension, a similar pattern of global Cd burial fluxes in organic matter, sulfides, etc., which are also suggested by other Cd isotope studies in the Xiaotan and Zhongnancun sections (Frei et al., 2020; 2021; Frederiksen et al., 2022a; Hohl et al., 2019). Actually, the similarity of organic matter fluxes in the early Cambrian and modern oceans are also supported by nitrogen cycles (Wang et al., 2018). Sufficient nutrient supply, together with higher oxygen concentrations,

may have supported efficient aerobic respiration to provide energy for energetically expensive behaviours, such as active muscular carnivory, locomotion, and bioturbation, and lead to the appearance of large and complex animals and ecological dominance of the characteristic Cambrian fauna (Sperling et al., 2013).

Ocean anoxia in the latest Ediacaran might be linked with the late Ediacaran mass extinction event, and the subsequent stepwise oxygenation of the deep-water in the Nanhua basin over the E–C transition might have expanded the habitat area for marine fauna. The inferred Cambrian seawater Cd isotope value is comparable to the modern deep ocean, indicating a modern-esque bio-productivity level in the Cambrian Nanhua ocean that could have been facilitated by elevated nutrient inputs from weathering of continental landmasses. This inference is supported by Cr, Mo and U isotope data measured the same sedimentary succession (e.g., Lehmann et al., 2016; Xu et al., 2023). Sufficient nutrient supply with rising oxygen content of the ocean could have helped trigger the Cambrian radiation of animals.

6. Conclusion

The cadmium isotope composition ($\delta^{114}\text{Cd}$) of the ZK4411 core in South China shows secular variation (-0.70‰ to $+0.35\text{‰}$) throughout the Ediacaran–Cambrian transition. This wide range of variation is controlled by a combination of local redox factors controlling Cd burial phases and global-scale changes in the Cd cycle. The rapid positive $\delta^{114}\text{Cd}$ shift in the latest Ediacaran might represent local anoxia, which could be linked with the late Ediacaran mass extinction. The subsequent shift to lighter $\delta^{114}\text{Cd}$ values might indicate oxygenation of the ocean in the Nanhua basin during the E–C transition. The ocean oxygenation could have expanded the habitat area for marine fauna and provided the oxygen necessary for large body size animals and energetically expensive activities. The heaviest Cd isotope composition recorded in the early Cambrian ($+0.28 \pm 0.12\text{‰}$, $n = 3$) is similar to that of the modern deep ocean ($+0.25 \pm 0.04\text{‰}$), suggesting their similarity in global Cd cycling, and in terms of organic matter, similar organic-Cd burial rates and primary productivity levels. The increased oxygen levels in Earth's surface environments and elevated bio-limiting nutrients in the oceans may have expanded the habitable regions of the ocean and supported the diversification of animal life.

CRediT authorship contribution statement

Zeyang Liu: Writing – original draft, Investigation, Funding acquisition, Conceptualization. **Alexander J. Dickson:** Writing – review & editing, Funding acquisition, Data curation, Conceptualization. **Haijing Sun:** Writing – review & editing, Formal analysis, Conceptualization. **Yaowen Wu:** Formal analysis. **Zhen Qiu:** Investigation, Formal analysis, Data curation. **Hui Tian:** Writing – review & editing, Supervision, Resources, Funding acquisition, Data curation, Conceptualization.

Declaration of competing interest

The authors declare that they have no known competing financial interests or personal relationships that could have appeared to influence the work reported in this paper.

Data availability

All data analysed during this study are included in this published article (and its supplementary materials).

Acknowledgements

The editor Prof. Vasileios Mavromatis, Lukas Ackerman, and one anonymous reviewer are thanked for their comments and suggestions that have greatly enhanced the whole quality and clarity of this

manuscript. We gratefully acknowledge the Natural Science Foundation of China (NSFC Grant No. 41925014 to H.T., 42303056 to Z.L., 42222209 to Z.Q., 42203057 to Y.W.), and the Natural Science Foundation of Sichuan Province (23NSFC5461 to Z.L.). A.J.D. acknowledges funding from UKRI Frontier Research grant DISTILL (EP/X022080/1). This is contribution No. IS-3533 from GIGCAS.

Appendix A. Supplementary data

Supplementary data to this article can be found online at <https://doi.org/10.1016/j.chemgeo.2024.122275>.

References

- Abouchami, W., Galer, S.J.G., Horner, T.J., Rehkämper, M., Wombacher, F., Xue, Z., Lambelet, M., Gault-Ringold, M., Stirling, C.H., Schönbacher, M., Shiel, A.E., Weis, D., Holdship, P.F., 2012. A Common Reference Material for Cadmium Isotope Studies – NIST SRM 3108. *Geostand. Geoanal. Res.* 37, 5–17.
- Brasier, M.D., Lindsay, J.F., 2001. Did supercontinental amalgamation trigger the “Cambrian explosion”? In: Zhuravlev, A.Y., Riding, R. (Eds.), *The Ecology of the Cambrian Radiation*. Columbia University Press, New York, pp. 69–89.
- Bridgestock, L., Rehkämper, M., van de Fliedert, T., Murphy, K., Khondoker, R., Baker, A.R., Chance, R., Strelkopytov, S., Humphreys-Williams, E., Achterberg, E.P., 2017. The Cd isotope composition of atmospheric aerosols from the Tropical Atlantic Ocean. *Geophys. Res. Lett.* 44, 2932–2940.
- Bruland, K.W., 1980. Oceanographic distributions of cadmium, zinc, nickel, and copper in the North Pacific. *Earth Planet. Sci. Lett.* 47, 176–198.
- Bryan, A.L., Dickson, A.J., Dowdall, F., Murphy, K., Porcelli, D., Henderson, G.M., 2021. Controls on the cadmium isotope composition of modern marine sediments. *Earth Planet. Sci. Lett.* 565, 116946.
- Canfield, D.E., Poulton, S.W., Knoll, A.H., Narbonne, G.M., Ross, G., Goldberg, T., Strauss, H., 2008. Ferruginous Conditions Dominated later Neoproterozoic Deep-Water Chemistry. *Science* 321, 949–952.
- Charvet, J., 2013. The Neoproterozoic–Early Paleozoic tectonic evolution of the South China Block: An overview. *J. Asian Earth Sci.* 74, 198–209.
- Chen, X., Ling, H.-F., Vance, D., Shields-Zhou, G.A., Zhu, M., Poulton, S.W., Och, L.M., Jiang, S.-Y., Li, D., Cremonese, L., Archer, C., 2015. Rise to modern levels of ocean oxygenation coincided with the Cambrian radiation of animals. *Nat. Commun.* 6, 7142.
- Chen, L., Little, S.H., Kreissig, K., Severmann, S., McManus, J., 2021. Isotopically Light Cd in Sediments underlying Oxygen Deficient zones. *Front. Earth Sci.* 9.
- Condon, D., Zhu, M., Bowring, S., Wang, W., Yang, A., Jin, Y., 2005. U–Pb Ages from the Neoproterozoic Doushantuo Formation, China. *Science* 308, 95–98.
- Conway, T.M., John, S.G., 2015. Biogeochemical cycling of cadmium isotopes along a high-resolution section through the North Atlantic Ocean. *Geochim. Cosmochim. Acta* 148, 269–283.
- Cumming, V.M., Selby, D., Lillis, P.G., 2012. Re–Os geochronology of the lacustrine Green River Formation: Insights into direct depositional dating of lacustrine successions, Re–Os systematics and paleocontinental weathering. *Earth Planet. Sci. Lett.* 359, 194–205.
- Dickson, A.J., Idiz, E., Porcelli, D., van den Boorn, S.H.J.M., 2020. The influence of thermal maturity on the stable isotope compositions and concentrations of molybdenum, zinc and cadmium in organic-rich marine mudrocks. *Geochim. Cosmochim. Acta* 287, 205–220.
- Dickson, A.J., Idiz, E., Porcelli, D., Murphy, M.J., Celestino, R., Jenkyns, H.C., Poulton, S.W., Hesselbo, S.P., Hooker, J.N., Ruhl, M., van den Boorn, S.H.J.M., 2022. No effect of thermal maturity on the Mo, U, Cd, and Zn isotope compositions of lower Jurassic organic-rich sediments. *Geology* 50, 598–602.
- Droser, M.L., Gehling, J.G., 2015. The advent of animals: the view from the Ediacaran. *Proc. Natl. Acad. Sci.* 112, 4865–4870.
- Druce, M., Stirling, C.H., Bostock, H.C., Rolison, J.M., 2022. Examining the effects of chemical cleaning, leaching, and partial dissolution on zinc and cadmium isotope fractionation in marine carbonates. *Chem. Geol.* 592, 120738.
- Fan, H., Wen, H., Zhu, X., Hu, R., Tian, S., 2013. Hydrothermal activity during Ediacaran–Cambrian transition: Silicon isotopic evidence. *Precambrian Res.* 224, 23–35.
- Frederiksen, J.A., Klæbe, R.M., Farkaš, J., Swart, P.K., Frei, R., 2022a. Cadmium isotopes in Bahamas platform carbonates: a base for reconstruction of past surface water bioproductivity and their link with chromium isotopes. *Sci. Total Environ.* 806, 150565.
- Frederiksen, J.A., Wei, W., Rugen, E.J., Ling, H.-F., Frei, R., 2022b. Cadmium isotopes in Late Ediacaran–Early Cambrian Yangtze Platform carbonates – Reconstruction of bioproductivity in ambient surface seawater. *Palaeogeogr. Palaeoclimatol. Palaeoecol.* 601, 111096.
- Frederiksen, J.A., Thibault, N., Gilleaudeau, G.J., Bjerrum, C.J., Moreau, J., Frei, R., 2024. Combined cadmium and chromium isotopes record a collapse of bioproductivity across the Cretaceous–Paleogene boundary in the Danish basin. *Chem. Geol.* 654, 122058.
- Frei, R., Lehmann, B., Xu, L., Frederiksen, J.A., 2020. Surface water oxygenation and bioproductivity – a link provided by combined chromium and cadmium isotopes in early Cambrian metalliferous black shales (Nanhua Basin, South China). *Chem. Geol.* 552, 119785.

- Frei, R., Xu, L., Frederiksen, J.A., Lehmann, B., 2021. Signals of combined chromium-cadmium isotopes in basin waters of the Early Cambrian - Results from the Maoshi and Zhijin sections, Yangtze Platform, South China. *Chem. Geol.* 563, 120061.
- Guinoiseau, D., Galer, S.J.G., Abouchami, W., 2018. Effect of cadmium sulphide precipitation on the partitioning of Cd isotopes: Implications for the oceanic Cd cycle. *Earth Planet. Sci. Lett.* 498, 300–308.
- Guinoiseau, D., Galer, S.J.G., Abouchami, W., Frank, M., Achterberg, E.P., Haug, G.H., 2019. Importance of Cadmium Sulfides for Biogeochemical Cycling of Cd and its Isotopes in Oxygen Deficient Zones—a Case Study of the Angola Basin. *Glob. Biogeochem. Cycles* 33, 1746–1763.
- He, T., Zhu, M., Mills, B.J.W., Wynn, P.M., Zhuravlev, A.Y., Tostevin, R., Pogge von Strandmann, P.A.E., Yang, A., Poulton, S.W., Shields, G.A., 2019. Possible links between extreme oxygen perturbations and the Cambrian radiation of animals. *Nat. Geosci.* 12, 468–474.
- Ho, T.-Y., Quigg, A., Finkel, Z.V., Milligan, A.J., Wyman, K., Falkowski, P.G., Morel, F.M.M., 2003. The Elemental Composition of some Marine Phytoplankton. *J. Phycol.* 39, 1145–1159.
- Hohl, S.V., Jiang, S.-Y., Wei, H.-Z., Pi, D.-H., Liu, Q., Viehmann, S., Galer, S.J.G., 2019. Cd isotopes trace periodic (bio)geochemical metal cycling at the verge of the Cambrian animal evolution. *Geochim. Cosmochim. Acta* 263, 195–214.
- Horner, T.J., Rickaby, R.E.M., Henderson, G.M., 2011. Isotopic fractionation of cadmium into calcite. *Earth Planet. Sci. Lett.* 312, 243–253.
- Janssen, D.J., Conway, T.M., John, S.G., Christian, J.R., Kramer, D.L., Pedersen, T.F., Cullen, J.T., 2014. Undocumented water column sink for cadmium in open ocean oxygen-deficient zones. *Proc. Natl. Acad. Sci.* 111, 6888–6893.
- Janssen, D.J., Abouchami, W., Galer, S.J.G., Cullen, J.T., 2017. Fine-scale spatial and interannual cadmium isotope variability in the subarctic Northeast Pacific. *Earth Planet. Sci. Lett.* 472, 241–252.
- Janssen, D.J., Abouchami, W., Galer, S.J.G., Purdon, K.B., Cullen, J.T., 2019. Particulate cadmium stable isotopes in the subarctic northeast Pacific reveal dynamic Cd cycling and a new isotopically light Cd sink. *Earth Planet. Sci. Lett.* 515, 67–78.
- Jiang, G., Sohl, L.E., Christie-Blick, N., 2003. Neoproterozoic stratigraphic comparison of the Lesser Himalaya (India) and Yangtze block (South China): Paleogeographic implications. *Geology* 31, 917–920.
- Jiang, G., Kennedy, M.J., Christie-Blick, N., Wu, H., Zhang, S., 2006. Stratigraphy, Sedimentary Structures, and Textures of the late Neoproterozoic Doushantuo Cap Carbonate in South China. *J. Sediment. Res.* 76, 978–995.
- Jiang, S.-Y., Yang, J.-H., Ling, H.-F., Chen, Y.-Q., Feng, H.-Z., Zhao, K.-D., Ni, P., 2007. Extreme enrichment of polymetallic Ni–Mo–PGE–Au in lower Cambrian black shales of South China: an Os isotope and PGE geochemical investigation. *Palaeogeogr. Palaeoclimatol. Palaeoecol.* 254, 217–228.
- Jiang, G., Shi, X., Zhang, S., Wang, Y., Xiao, S., 2011. Stratigraphy and paleogeography of the Ediacaran Doushantuo Formation (ca. 635–551Ma) in South China. *Gondwana Res.* 19, 831–849.
- Lacan, F., Francois, R., Ji, Y., Sherrell, R.M., 2006. Cadmium isotopic composition in the ocean. *Geochim. Cosmochim. Acta* 70, 5104–5118.
- Laflamme, M., Darroch, S.A.F., Tweedt, S.M., Peterson, K.J., Erwin, D.H., 2013. The end of the Ediacara biota: Extinction, biotic replacement, or Cheshire Cat? *Gondwana Res.* 23, 558–573.
- Lambelet, M., Rehkämper, M., van de Fliedert, T., Xue, Z., Kreissig, K., Coles, B., Porcelli, D., Andersson, P., 2013. Isotopic analysis of Cd in the mixing zone of Siberian rivers with the Arctic Ocean—New constraints on marine Cd cycling and the isotope composition of riverine Cd. *Earth Planet. Sci. Lett.* 361, 64–73.
- Lehmann, B., Nägler, T.F., Holland, H.D., Wille, M., Mao, J., Pan, J., Ma, D., Dulski, P., 2007. Highly metalliferous carbonaceous shale and early Cambrian seawater. *Geology* 35 (5), 403–406. <https://doi.org/10.1130/g23543a.1>.
- Lehmann, B., Frei, R., Xu, L., Mao, J., 2016. Early Cambrian Black Shale-Hosted Mo-Ni and V Mineralization on the Rifted margin of the Yangtze Platform, China: Reconnaissance Chromium Isotope Data and a Refined Metallogenic Model. *Econ. Geol.* 111 (1), 89–103. <https://doi.org/10.2113/econgeo.111.1.89>.
- Li, Z.-X., Li, X.H., Kinny, P.D., Wang, J., 1999. The breakup of Rodinia: did it start with a mantle plume beneath South China? *Earth Planet. Sci. Lett.* 173, 171–181.
- Li, C., Shi, W., Cheng, M., Jin, C., Algeo, T.J., 2020. The redox structure of Ediacaran and early Cambrian oceans and its controls. *Sci. Bull.* 65, 2141–2149.
- Liu, P., Yin, C., Chen, S., Tang, F., Gao, L., 2013. The biostratigraphic succession of acanthomorphic acritarchs of the Ediacaran Doushantuo Formation in the Yangtze Gorges area, South China and its biostratigraphic correlation with Australia. *Precambrian Res.* 225, 29–43.
- Middag, R., van Heuven, S.M.A.C., Bruland, K.W., de Baar, H.J.W., 2018. The relationship between cadmium and phosphate in the Atlantic Ocean unravelled. *Earth Planet. Sci. Lett.* 492, 79–88.
- Och, L.M., Shields-Zhou, G.A., Poulton, S.W., Manning, C., Thirlwall, M.F., Li, D., Chen, X., Ling, H., Osborn, T., Cremonese, L., 2013. Redox changes in early Cambrian black shales at Xiaotan section, Yunnan Province, South China. *Precambrian Res.* 225, 166–189.
- Och, L.M., Cremonese, L., Shields-Zhou, G.A., Poulton, S.W., Struck, U., Ling, H., Li, D., Chen, X., Manning, C., Thirlwall, M., Strauss, H., Zhu, M., 2016. Palaeoceanographic controls on spatial redox distribution over the Yangtze Platform during the Ediacaran–Cambrian transition. *Sedimentology* 63, 378–410.
- Pickard, H., Palk, E., Schönbacher, M., Moore, R.E.T., Coles, B.J., Kreissig, K., Nilsson-Kerr, K., Hammond, S.J., Takazawa, E., Hémond, C., Tropper, P., Barfod, D.N., Rehkämper, M., 2022. The cadmium and zinc isotope compositions of the silicate Earth – Implications for terrestrial volatile accretion. *Geochim. Cosmochim. Acta* 338, 165–180.
- Plass, A., Schlosser, C., Sommer, S., Dale, A.W., Achterberg, E.P., Scholz, F., 2020. The control of hydrogen sulfide on benthic iron and cadmium fluxes in the oxygen minimum zone off Peru. *Biogeosciences* 17, 3685–3704.
- Plass, A., Dale, A.W., Scholz, F., 2021. Sedimentary cycling and benthic fluxes of manganese, cobalt, nickel, copper, zinc and cadmium in the Peruvian oxygen minimum zone. *Mar. Chem.* 233, 103982.
- Quay, P., Cullen, J., Landing, W., Morton, P., 2015. Processes controlling the distributions of Cd and PO₄ in the ocean. *Glob. Biogeochem. Cycles* 29, 830–841.
- Rehkämper, M., Wombacher, F., Horner, T.J., Xue, Z., 2012. Natural and Anthropogenic Cd Isotope Variations. In: Baskaran, M. (Ed.), *Handbook of Environmental Isotope Geochemistry*, vol. I. Springer Berlin Heidelberg, Berlin, Heidelberg, pp. 125–154.
- Ripperger, S., Rehkämper, M., Porcelli, D., Halliday, A.N., 2007. Cadmium isotope fractionation in seawater — a signature of biological activity. *Earth Planet. Sci. Lett.* 261, 670–684.
- Rosenthal, Y., Lam, P., Boyle, E.A., Thomson, J., 1995. Authigenic cadmium enrichments in suboxic sediments: Precipitation and postdepositional mobility. *Earth Planet. Sci. Lett.* 132, 99–111.
- Rudnick, R.L., Gao, S., 2003. 3.01 - Composition of the Continental Crust. In: Holland, H. D., Turekian, K.K. (Eds.), *Treatise on Geochemistry*. Pergamon, Oxford, pp. 1–64.
- Sahoo, S.K., Planavsky, N.J., Jiang, G., Kendall, B., Owens, J.D., Wang, X., Shi, X., Anbar, A.D., Lyons, T.W., 2016. Oceanic oxygenation events in the anoxic Ediacaran. *Geobiology* 14, 457–468.
- Schmitt, A.-D., Galer, S.J.G., Abouchami, W., 2009. Mass-dependent cadmium isotopic variations in nature with emphasis on the marine environment. *Earth Planet. Sci. Lett.* 277, 262–272.
- Shields, G.A., 2016. Earth system transition during the Tonian–Cambrian interval of biological innovation: nutrients, climate, oxygen and the marine organic carbon capacitor. *Geol. Soc. Lond. Spec. Publ.* 448, 161–177.
- Sieber, M., Conway, T.M., de Souza, G.F., Obata, H., Takano, S., Sohrin, Y., Vance, D., 2019. Physical and biogeochemical controls on the distribution of dissolved cadmium and its isotopes in the Southwest Pacific Ocean. *Chem. Geol.* 511, 494–509.
- Sieber, M., Lanning, N.T., Bunnell, Z.B., Bian, X., Yang, S.-C., Marsay, C.M., Landing, W. M., Buck, C.S., Fitzsimmons, J.N., John, S.G., Conway, T.M., 2023. Biological, Physical, and Atmospheric Controls on the distribution of Cadmium and its Isotopes in the Pacific Ocean. *Glob. Biogeochem. Cycles* 37 e2022GB007441.
- Sperling, E.A., Frieder, C.A., Raman, A.V., Girguis, P.R., Levin, L.A., Knoll, A.H., 2013. Oxygen, ecology, and the Cambrian radiation of animals. *Proc. Natl. Acad. Sci.* 110, 13446–13451.
- Sperling, E.A., Wolock, C.J., Morgan, A.S., Gill, B.C., Kunzmann, M., Halverson, G.P., Macdonald, F.A., Knoll, A.H., Johnston, D.T., 2015. Statistical analysis of iron geochemical data suggests limited late Proterozoic oxygenation. *Nature* 523, 451–454.
- Squire, R.J., Campbell, I.H., Allen, C.M., Wilson, C.J.L., 2006. Did the Transgondwanan supermountain trigger the explosive radiation of animals on Earth? *Earth Planet. Sci. Lett.* 250, 116–133.
- Steiner, M., Wallis, E., Erdtmann, B.-D., Zhao, Y., Yang, R., 2001. Submarine-hydrothermal exhalative ore layers in black shales from South China and associated fossils — insights into a lower Cambrian facies and bio-evolution. *Palaeogeogr. Palaeoclimatol. Palaeoecol.* 169, 165–191.
- Sun, W., Zuo, Y., Lin, Z., Wu, Z., Liu, H., Lin, J., Chen, B., Chen, Q., Pan, C., Lan, B., Liu, S., 2023. Impact of tectonic deformation on shale pore structure using adsorption experiments and 3D digital core observation: a case study of the Niutian Formation in Northern Guizhou. *Energy* 278, 127724.
- Sweere, T., van den Boorn, S., Dickson, A.J., Reichart, G.-J., 2016. Definition of new trace-metal proxies for the controls on organic matter enrichment in marine sediments based on Mn, Co, Mo and Cd concentrations. *Chem. Geol.* 441, 235–245.
- Sweere, T.C., Dickson, A.J., Jenkyns, H.C., Porcelli, D., Ruhl, M., Murphy, M.J., Idiz, E., van den Boorn, S.H.J.M., Eldrett, J.S., Henderson, G.M., 2020. Controls on the Cd-isotope composition of Upper cretaceous (Cenomanian–Turonian) organic-rich mudrocks from South Texas (Eagle Ford Group). *Geochim. Cosmochim. Acta* 287, 251–262.
- Tan, D., Zhu, J.-M., Wang, X., Han, G., Lu, Z., Xu, W., 2020. High-sensitivity determination of Cd isotopes in low-Cd geological samples by double spike MC-ICP-MS. *J. Anal. At. Spectrom.* 35, 713–727.
- Tostevin, R., Mills, B.J.W., 2020. Reconciling proxy records and models of Earth's oxygenation during the Neoproterozoic and Palaeozoic. *Interface Focus* 10, 20190137.
- Tostevin, R., Clarkson, M.O., Gangl, S., Shields, G.A., Wood, R.A., Bowyer, F., Penny, A. M., Stirling, C.H., 2019. Uranium isotope evidence for an expansion of anoxia in terminal Ediacaran oceans. *Earth Planet. Sci. Lett.* 506, 104–112.
- Wang, J., Li, Z.-X., 2003. History of Neoproterozoic rift basins in South China: implications for Rodinia break-up. *Precambrian Res.* 122, 141–158.
- Wang, D., Ling, H.-F., Struck, U., Zhu, X.-K., Zhu, M., He, T., Yang, B., Gamper, A., Shields, G.A., 2018. Coupling of ocean redox and animal evolution during the Ediacaran–Cambrian transition. *Nat. Commun.* 9, 2575.
- Wei, G.-Y., Planavsky, N.J., Tarhan, L.G., Chen, X., Wei, W., Li, D., Ling, H.-F., 2018. Marine redox fluctuation as a potential trigger for the Cambrian explosion. *Geology* 46, 587–590.
- Wen, H., Carignan, J., Zhang, Y., Fan, H., Cloquet, C., Liu, S., 2011. Molybdenum isotopic records across the Precambrian–Cambrian boundary. *Geology* 39, 775–778.
- Wen, H., Zhu, C., Zhang, Y., Cloquet, C., Fan, H., Fu, S., 2016. Zn/Cd ratios and cadmium isotope evidence for the classification of lead-zinc deposits. *Sci. Rep.* 6 (1), 25273. <https://doi.org/10.1038/srep25273>.
- Wu, Y., 2021. The Developmental Mechanisms of OM-Rich Shale during the Ediacaran–Cambrian Transition in the Upper Yangtze Block and its Implications for Nitrogen-

- Rich Shale Gas. University of Chinese Academy of Sciences. PhD thesis. (in Chinese with English abstract).
- Wu, Y., Tian, H., Li, J., Li, T., Ji, S., 2021. Reconstruction of oceanic redox structures during the Ediacaran-Cambrian transition in the Yangtze Block of South China: Implications from Mo isotopes and trace elements. *Precambrian Res.* 359, 106181.
- Wu, Y., Tian, H., Jia, W., Li, J., Li, T., Zhou, Q., Xie, L., Peng, P.A., 2022. Nitrogen isotope evidence for stratified ocean redox structure during late Ediacaran to Cambrian Age 3 in the Yangtze Block of South China. *Chem. Geol.* 589, 120679.
- Xiang, L., Schoepfer, S.D., Shen, S.-Z., Cao, C.-Q., Zhang, H., 2017. Evolution of oceanic molybdenum and uranium reservoir size around the Ediacaran–Cambrian transition: Evidence from western Zhejiang, South China. *Earth Planet. Sci. Lett.* 464, 84–94.
- Xu, L., Lehmann, B., Weyer, S., Wen, H., Mao, J., Neubert, N., Jian, W., 2023. Inverse Mo versus U isotope correlation of early Cambrian highly metalliferous black shales in South China indicates synsedimentary metal enrichment from a near-modern ocean. *Mineral. Deposita* 59, 155–167.
- Yang, C., Li, X.-H., Li, Z.-X., Zhu, M., Lu, K., 2020. Provenance Evolution of Age-Calibrated Strata reveals when and how South China Block Collided with Gondwana. *Geophys. Res. Lett.* 47 e2020GL090282.
- Yi, Y., Chen, F., Algeo, T.J., Feng, Q., 2022. Deep-water fossil assemblages from the Ediacaran-Cambrian transition of western Hunan, South China and their biostratigraphic and evolutionary implications. *Palaeogeogr. Palaeoclimatol. Palaeoecol.* 591, 110878.
- Zhang, X., Shu, D., 2021. Current understanding on the Cambrian Explosion: questions and answers. *PalZ* 95, 641–660.
- Zhang, S., Jiang, G., Zhang, J., Song, B., Kennedy, M.J., Christie-Blick, N., 2005. U-Pb sensitive high-resolution ion microprobe ages from the Doushantuo Formation in South China: Constraints on late Neoproterozoic glaciations. *Geology* 33, 473–476.
- Zhang, F., Xiao, S., Kendall, B., Romaniello, S.J., Cui, H., Meyer, M., Gilleaudeau, G.J., Kaufman, A.J., Anbar, A.D., 2018. Extensive marine anoxia during the terminal Ediacaran Period. *Sci. Adv.* 4, eaan8983.
- Zhao, K., Zhu, G., Li, T., Chen, Z., Li, S., 2023. Fluctuations of continental chemical weathering control primary productivity and redox conditions during the Earliest Cambrian. *Geol. J.* 58, 3659–3672.
- Zhong, Q.-H., Yin, L., Li, J., Feng, Y.-X., Shen, N.-P., Peng, B.-Y., Wang, Z.-Y., 2023. A single-stage anion exchange separation method for Cd isotopic analysis in geological and environmental samples by MC-ICP-MS. *J. Anal. At. Spectrom.* 38, 2291–2301.
- Zhu, M., Zhuravlev, A.Y., Wood, R.A., Zhao, F., Sukhov, S.S., 2017. A deep root for the Cambrian explosion: Implications of new bio- and chemostratigraphy from the Siberian Platform. *Geology* 45, 459–462.